Betulinic acid decreases lipid accumulation in adipogenesis-induced human mesenchymal stem cells with upregulation of *PGC-1α* and *UCP-1* and post-transcriptional downregulation of adiponectin and leptin secretion

Sasithon Senamontree[1], Thitiporn Lakthan[1], Pornsri Charoenpanich[2], Chanpen Chanchao[3] and Adisri Charoenpanich[1]

[1] Department of Biology, Faculty of Science, Silpakorn University, Nakhon Pathom, Thailand
[2] Department of Food Technology, Faculty of Engineering and Industrial Technology, Silpakorn University, Nakhon Pathom, Thailand
[3] Department of Biology, Faculty of Science, Chulalongkorn University, Bangkok, Thailand

Corresponding author
Adisri Charoenpanich,
Charoenpanich_a@silpakorn.edu

ABSTRACT

Background: Controlling cellular functions, including stem cell growth and differentiation, can be the key for the treatment of metabolic disorders, such as type II diabetes mellitus (T2DM). Previously identified as peroxisome proliferator-activated receptor gamma (*PPARγ*) antagonist, betulinic acid (BA) may have the capability to control stem cell homeostasis, benefiting T2DM treatment. In this study, the effects of BA on osteogenesis and adipogenesis mechanisms of human mesenchymal stem cells (hMSCs) were investigated.

Results: We observed that BA increased hMSC osteogenesis by enhancing the alkaline phosphatase activity, calcium deposition, and mRNA expressions of osteogenic markers, namely, runt-related transcription factor 2, osteocalcin, and osteopontin. In addition, BA decreased hMSC adipogenesis with the decrease in glycerol-3-phosphate dehydrogenase activity, reduced intracellular lipid accumulations, down-regulated CCAAT-enhancer-binding protein alpha, and suppressed post-transcriptional adiponectin and leptin secretion. BA increased the brown adipocyte characteristics with the increase in the ratio of small lipid droplets and glucose uptake. Furthermore, the mRNA expressions of brown adipocyte markers, namely, *PPARγ* coactivator one alpha, uncoupling protein 1, and interleukin-6 increased.

Conclusions: Our results uncovered the mechanisms of how BA improved glucose and lipid metabolisms by decreasing white adipogenesis and increasing brown adipogenesis. Altogether, BA may be used for balancing glucose metabolisms without the potential side effects on bone loss or weight gain.

INTRODUCTION

Human mesenchymal stem cells (hMSCs) are progenitor cells of mesenchymal lineage tissues, including muscle, cartilage, bone, and fat. Within these tissues, several of the hMSCs are left as undifferentiated adult stem cells. These undifferentiated hMSCs in adults maintain their crucial roles in balancing tissue homeostasis and controlling their surrounding microenvironments (*Chamberlain et al., 2007*; *Charoenpanich et al., 2011*; *Samuel et al., 2019*). In particular, bone and adipose tissues are dynamic tissues that can be dramatically altered by physical activity, lifestyle behavior, and diet. The overexpansion of adipose tissue in obesity has an inverse effect on bone metabolisms by decreasing bone formation through the competitive utilization of the same mesenchymal progenitor cells and increasing bone resorption by inducing osteoclast activation with pro-inflammatory cytokine secretion (*Abdallah, 2017*; *Cao, 2011*; *James, 2013*; *Lacey et al., 2009*; *Sonowal et al., 2013*). Furthermore, the crosstalk between osteogenesis and adipogenesis can complicate metabolic disorders, such as diabetes mellitus, as evidenced in the case of type II diabetes mellitus (T2DM) treatments (*Grey, 2009*; *Sardone et al., 2011*). Further, patients with type I and T2DM also display the risk of osteoporotic fracture (*Sellmeyer et al., 2016*).

Betulinic acid (BA) is a naturally occurring pentacyclic triterpenoid with potential anti-obesity, anti-diabetes, anti-inflammation, and anti-osteoporosis properties (*Kim et al., 2019*; *Ou et al., 2019*; *Park et al., 2014*; *Song et al., 2021*). The treatment with BA at 10 and 30 mg/kg can restore the imbalance of inflammatory mediators (tumor necrosis factor alpha (TNF-α), interleukin 6 (IL-6), and IL-10) and prevent cecal ligation and puncture-induced kidney damage in mice (*Lingaraju et al., 2015*). The anti-inflammatory activity of BA through modulating TNF-α production by macrophages with IL-10-dependent mechanism was also reported in a lethal dose of lipopolysaccharide-treated BALB/c mice (*Costa et al., 2014*). Another anti-inflammation signaling pathway triggered by BA is through the activation of peroxisome proliferator-activated receptor gamma (PPARγ) as shown in the IL-1β-induced inflammation of osteoarthritis chondrocytes (*Jingbo et al., 2015*). PPARγ is the master regulator of adipogenesis and the target of insulin-sensitizing drug, thiazolidinediones (TZDs) (*Kubota et al., 2006*; *Lehmann et al., 1995*; *Murakami-Nishida et al., 2019*).

An *in vivo* study of mice fed with a high-fat diet (HFD) showed that BA prevented abdominal fat accumulation with the decrease in blood glucose, plasma triglycerides, and total cholesterol (*de Melo et al., 2009*). A study on African medicinal plant extract, *Diospyros bipindensis*, showed that BA had a high affinity to PPARγ and acted as PPARγ antagonist, which induced glucose uptake, inhibited adipogenesis in murine pre-adipocyte (3T3-L1 cells), and enhanced osteogenesis in murine pre-osteoblast (MC3T3-E1) (*Brusotti et al., 2017*). An *in vitro* study of MC3T3-E1 cells showed that BA enhanced osteogenesis through bone morphogenetic protein(BMP)/runt-related transcription factor 2 (RUNX2) and β-catenin signals (*Lo et al., 2010*). We hypothesized that BA can be a potent agent that triggers the balance of bone and adipose tissue formation in progenitor cells. Here, we addressed the mechanisms of BA triggering the balance between

osteogenesis and adipogenesis in hMSCs. We reported that BA can increase hMSC osteogenesis and suppress hMSC adipogenesis. Additionally, we proposed that the suppression of adipogenesis by BA with increases in metabolic activity and glucose uptake might be through inducing brown fat formation in hMSCs.

MATERIALS & METHODS

Cell culture

hMSCs were obtained from the Japanese Collection of Research Bioresources Cell Bank (JCRB Cell Bank, UE7T-13, JCRB1154, Lot #07072007). This hMSC cell line had been established for its multipotent differentiation, including osteogenesis and adipogenesis (*Tsujimura, Kusamori & Nishikawa, 2019*; *Zhang et al., 2019*). For cell proliferation, hMSCs were cultured in complete growth media (CGM: α-Minimum Essential Medium with 10% fetal bovine serum, 100 units/ml Penicillin-Streptomycin, and two mM L-glutamine) at 37 °C and 5% CO_2. The medium was changed every 3 days, and the cells were sub-cultured after about 80% confluency. For cell differentiation, hMSCs were seeded in multi-well plates. When 80% confluency was reached (within 2–3 days), the CGM was replaced with osteogenic medium (OM) or adipogenic medium (AM). BA was purchased from Sigma-Aldrich (cat#B8936) and initially dissolved in 50 mM dimethyl sulfoxide (DMSO). The final concentrations of DMSO were kept below 0.05% in all conditions.

Cell differentiation media

In this study, an OM recipe without dexamethasone was used to highlight the effect of BA. The OM is a CGM-based medium supplemented with 50 μM ascorbic acid and five mM β-glycerophosphate (*Choi et al., 2016*).

AM is also CGM-based with one μM dexamethasone, 10 μg/ml h-insulin, 100 μM indomethacin, and 500 μM isobutymethyxanthine (*Nöth et al., 2002*).

Metabolic activity of hMSCs

alamarBlue™ dye (Invitrogen) is a resazurin-based assay that can be used for continuous monitoring of mitochondrial function, and it was performed for the metabolic activity analysis of hMSCs as per manufacturer's instructions. For metabolic tracking, the cells were seeded at 5×10^3 cells/well in 96-well plates and treated with BA at 5, 10, 15, and 20 μM for 7 and 10 days in CGM, OM, or AM. At the designated time points, the medium was replaced with fresh CGM with 10% alamarBlue and then incubated for 2 h before absorbance reading at 570 and 600 nm. The percentage of metabolic activity was compared with the control group without BA at the selected time points for each media type (*Maxson & Burg, 2008*; *Quent et al., 2010*).

Evaluations of osteogenesis

The effects of BA on hMSC osteogenesis were evaluated in two levels, namely, alkaline phosphatase (ALP) enzymatic activity and bone matrix calcium deposition.

ALP is a critical enzyme in bone mineralization and known as an early marker of osteogenesis (*Mohamadnia et al., 2007*). For ALP activity assay, hMSCs were seeded at 5×10^3 cells/well in 96-well plates and cultured in OM for 7 days. The ALP activity assay was performed as previously described (*Montazerolghaem et al., 2016*). Briefly, the cells were lysed in a lysis buffer, followed by three freeze-thawing cycles to fully break the cells. A total of one mg/ml p-nitrophenyl phosphate substrate in diethanolamine was added to the cell lysis at the ratio of 2:1. The reactions were incubated at 37 °C, and the absorbance was read at 405 nm every 5 min for 30 min. The total protein was measured with bicinchoninic acid assay (*Walker, 1996*). The enzymatic activity was calculated as described in Enzymatic Assay of Alkaline Phosphatase, Diethanolamine Assay (EC 3. 1. 3. 1):

$$\text{Unit/mg protein} = \frac{\text{Unit/ml enzyme}}{\text{mg protein/ml enzyme}}$$

Calcium deposition was quantified with calcium colorimetric assay with o-cresolphthalein, which was adapted from the work of *Tu et al. (2014)*. Cells were seeded at 2×10^4 cells/well in 24-well plates and cultured in OM with 5, 10, 15, and 20 μM BA or control without BA in OM and CGM. After 14 days, the cells were washed twice with phosphate-buffered saline (PBS). Then, the accreted calcium was dissolved in 0.1 M HCl, shaken at 4 °C for 8 h, and centrifuged at 500×g for 2 min. The supernatant with dissolved calcium was then used for calcium quantification. A chromogenic reagent 190 μl (1.1 mM O-cresolphthalein complexone and 7.9 mM 8-hydroxyquinoline) was added to the 10 μl sample, and the absorbance was read at 570 nm.

To visualize the calcium nodule, we washed the cells twice with PBS, followed by 4% paraformaldehyde fixation for 10 min and staining with 2% alizarin red.

Evaluations of adipogenesis

The adipogenesis of hMSCs was analyzed with glycerol 3-phosphate dehydrogenase (GPDH) activity and intracellular lipid droplet accumulation.

Cell culture and cell lysate preparation for GPDH activity assay were performed with the same protocol as the ALP activity, but with the AM used for cell culture instead of an OM. Exactly 90 μl 334 μM b-nicotinamide adenine dinucleotide, which is the reduced form of NADH, was added to 100 μl cell lysate and then further incubated at 37 °C for 10 min before adding 10 μl four mM dihydroxyacetone phosphate. The absorbance was read at 340 nm every 5 min for 30 min. GPDH was calculated and normalized with the total protein (*Sottile & Seuwen, 2001*).

Oil Red O and Nile red staining were used to analyze the intracellular lipid accumulation. Oil Red O is a common oil droplet stain that can also be used to interpret the total triglyceride content by dissolving the dye for absorbance reading at 540 nm (*Kanawa et al., 2013*). hMSCs were cultured in an AM in 96-well plates for 21 days. Then, the cells were washed twice with PBS, followed by 4% paraformaldehyde fixation for 10 min. The oil droplets were stained with Oil Red O (1.8 mg/ml in 60% isopropanol)

for 10 min. The excess dye was then removed by washing with distilled water. The stained lipid was then dissolved in 100 µl isopropanol and read at 540 nm.

For the analysis of lipid droplet size and number, the cells were cultured in 48-well plates containing the AM for 21 days and then stained with 10 µg/ml Nile red (1% acetone in non-phenol red Dulbecco's Modified Eagle Medium) (*Hogan et al., 2016*). Images were captured with a fluorescence microscope (Olympus, CKX53) with the excitation wavelength at 495 nm, with five images obtained per well in triplicate and analyzed with ImageJ using function analyze the particles (*Deutsch et al., 2014*). Briefly, the images were binarized to black and white pixels. Then, watershedding techniques were applied to measure individual lipid droplets by size and perimeter.

Glucose uptake

The glucose uptake by hMSCs during adipogenesis was analyzed on days 10 and 14. Cells were seeded in 48-well plates at 1×10^4 cell/well. After 10 or 14 days, the medium was replaced with a fresh medium, and the glucose level was measured with Accu-chek guide (*Kim et al., 2018*) after 4 and 8 h.

Cellular mechanisms

mRNA gene expression analysis was performed with real-time reverse-transcription polymerase chain reaction (qRT-PCR). hMSCs were seeded in 24-well plates at 2×10^4 cell/well. The total RNA was extracted with Total RNA Mini Kit (Favorgen, FATRK001) and converted to cDNA with HyperScript^{TM} RT master mix with oligo dT (GeneAll, 601–703). The quantitative PCR was performed with the Applied Biosystems^{TM} 7,500 Real-Time PCR System using iTaq Universal SYBR Green Supermix (Biorad, 172–5,122). The PCR products were checked with melting temperature analysis. The ΔCT was calculated using GAPDH. The relative gene expressions were calculated using the $2^{-\Delta\Delta CT}$ method with the cut-off at twofold change and $P < 0.05$ (*Rao et al., 2013*). Table 1 shows the primer sequences.

The release of adipokines, adiponectin, IL-6, leptin, and TNF-α was measured with Milliplex Map Human Adipokine Magnetic Bead Panel Kit. hMSCs were seeded at 10^4 cells/well in 48-well plates. The culture medium was changed by half every 3 days and collected for cell-secreted adipokines on days 10, 14, and 17. The detection and analysis were performed in accordance with the manufacturer's instructions. At least 50 beads were counted for each replicate, and the results were calculated as pg/ml by comparison with the manufacturer's standard control (*Chen et al., 2014*).

Statistical analysis

All statistical analysis was performed with 27th edition of SPSS. Data are shown as mean ± standard deviation from three biological replicates. The Shapiro–Wilk test was applied to assess normality of the distributions. In cases of a normal distribution, one-way ANOVA with Tukey multiple comparison for equal variances or Dunnett's C multiple comparison for unequal variances were used. In cases of a non-normal distribution, the

Table 1 Primer sequences for qRT-PCR.

Gene	Forward (5–3′)	Reverse (5–3′)	Product length
Adiponectin	TCCTGCCAGTAACAGGGAAG	GGTTGGCGATTACCCGTTTG	89
ALP	CCCAAAGGCTTCTTCTTG	CTGGTAGTTGTTGTGAGC	357
β-catenin	GATTTGATGGAGTTGGACATGG	TGTTCTTGAGTGAAGGACTGAG	218
BMP2	ATGGATTCGTGGTGGAAGTG	GTGGAGTTCAGATGATCAGC	349
BMP7	GGTCATGAGCTTCGTCAACC	GCAGGAAGAGATCCGATTCC	236
C/EBP-α	AAGAAGTCGGTGGACAAGAACAG	TGCGCACCGCGATGT	70
FABP4	GCTTTGCCACCAGGAAAGTG	ATGGACGCATTCCACCACCA	281
GAPDH	GTTCCAATATGATTCCACCC	AGGGATGATGTTCTGGAGAG	487
GLUT-4	CTTCGAGACAGCAGGGGTAG	ACAGTCATCAGGATGGCACA	168
IL-6	GGTACATCCTCGACGGCATCT	GTGCCTCTTTGCTGCTTTCAC	81
Leptin	TCCCCTCTTGACCCATCTC	GGGAACCTTGTTCTGGTCAT	110
LEP-R	GCTATTTTGGGAAGATGT	TGCCTGGGCCTCTATCTC	499
MYF5	TTCTACGACGGCTCCTGCATA	CCACTCGCGGCACAAACT	67
OC	GGCGCTACCTGTATCAATGG	TCAGCCAACTCGTCACAGTC	106
OPN	CATGAGAATTGCAGTGATTTGCT	CTTGGAAGGGTCTGTGGGG	186
PGC-1α	GTTCCCGATCACCATATTCCA	GCGGTGTCTGTAGTGGCTTGA	101
PPARγ-2	CAGTGTGAATTACAGCAAACC	ACAGTGTATCAGTGAAGGAAT	101
PRDM16	CAGCACGGTGAAGCCATTC	GCGTGCATCCGCTTGTG	87
RUNX2	GTACAGCTTTAAGGATTCCCTCAATTC	TTGCTAATGCTTCGTGTTTCCA	86
TNF-α	CAGAGGGAAGAGTTCCCCAG	CCTTGGTCTGGTAGGAGACG	325
UCP-1	CTGGAATAGCGGCGTGCTT	AATAACACTGGACGTCGGGC	101
WNT3A	ACTACGTGGAGATCATGCCC	ATGAGCGTGTCACTGCAAAG	210

Kruskal–Wallis test with Mann Whitney U test was used to determine the level of significance between the groups. P values < 0.05 were accepted as significant.

RESULTS

BA increased the metabolic activity of hMSCs during adipogenesis

To track the changes in the metabolic activity of hMSCs in response to BA, we performed alamarBlue assays on days 7 and 10, proliferating phase, osteogenic differentiation, or adipogenic differentiation. The results showed that BA caused no alteration in the metabolic activity of hMSCs during the proliferating phase or osteogenic differentiation. The BA at 15, and 20 µM increased the metabolic activity of hMSCs during adipogenesis by 22% and 29%, respectively, on day 10 (Figs. 1A and 1B) without changes in total protein content (Fig. S1).

BA increased osteogenic differentiation and decreased adipogenic differentiation of hMSCs, changing calcium deposition, lipid accumulation, enzyme activities, and gene expressions

The effects of BA on hMSC osteogenesis or adipogenesis were investigated with enzyme activity assays, calcium deposition, or lipid accumulation. The results showed that ALP,
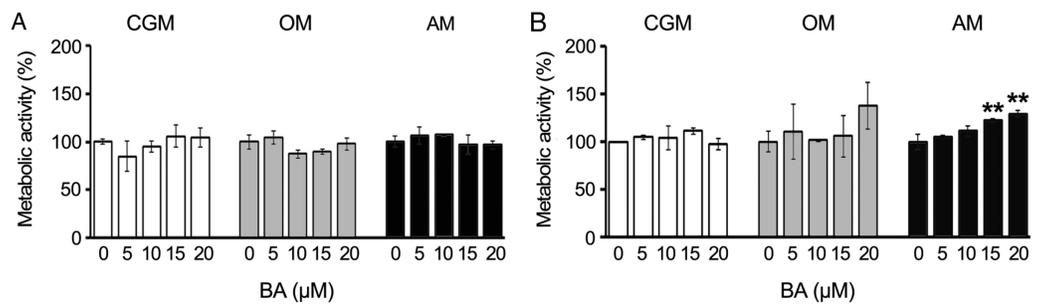
Figure 1 BA increased the metabolic activity of hMSCs during adipogenic differentiation. The metabolic activity of hMSCs was tracked with alamarBlue assay during the proliferating phase (CGM), osteogenic differentiation (OM), and adipogenic differentiation (AM) on days 7 (A) and 10 (B). $**P < 0.01$. Error bars represent standard deviation ($n = 3$).

the key enzyme in bone mineralization, significantly increased in hMSCs with a dose-dependent response to BA at 5–15 μM (Fig. 2A). At 15 μM, the ALP activity increased the most by 85%. Calcium accretion was also significantly increased by BA at 5, 10, and 15 μM as shown in the calcium quantification assay, with the average increase of about 4–5 μg/well or 15%–18% (Fig. 2B). With alizarin red staining, thicker and larger calcium nodules were observed in BA treatments at 5, 10, and 15 μM (Fig. 2C).

For hMSC adipogenesis, GPDH, the key enzyme in lipid biosynthesis, and its intracytoplasmical accumulation lipid were investigated. Our preliminary result showed elevated activity of GPDH in hMSCs by adipogenic induction at day 7 but not day 14 (Table S1). Day 7 was then selected as the timepoint for GPDH activity analysis. The results showed that BA at 5–20 μM significantly decreased the GPDH activity by 26%–34% (Fig. 2D). hMSC adipogenic differentiation was confirmed with Oil Red O staining (Fig. S2). At day 21, Oil Red O staining showed evident reduction in lipid accumulation with the decrease in total lipid content by 28%–45% (Figs. 2E and 2F).

BA can alter the hMSC lineage differentiations by enhancing bone formation with the increase in ALP enzymatic activity and bone matrix deposition and reducing fat cell formation with the demolishment of lipid droplet accumulation and GPDH enzyme activity.

Further, hMSC gene expression was analyzed with qRT-PCR. The effects of BA without additional differentiation supplements in the CGM were monitored on day 3. We observed that the effects of BA on hMSC early osteogenic gene expressions, namely *ALP*, β-catenin, and Wnt family member 3A (*WNT3A*) were not evident without osteogenic induction factors (Fig. 2G). However, the expression of adipogenic marker CCAAT-enhancer-binding proteins alpha (*C/EBP-α*) level was significantly reduced by BA alone (Fig. 2G). In addition, the remarkable downregulation of *C/EBP-α*, but not *PPARγ-2*, by BA was observed in hMSCs during adipogenic induction (Fig. 2H).

With osteogenic induction factors, BA significantly upregulated the expressions of late osteogenic markers, *ALP*, osteocalcin (*OC*), osteopontin (*OPN*), and *RUNX2* on day 14 (Fig. 2I). However, the expression of early osteogenic marker genes, *i.e.*, *ALP*, β-catenin, bone morphogenetic protein 2 (*BMP2*), *RUNX2*, and *WNT3A*, was not altered (Fig. 2I).
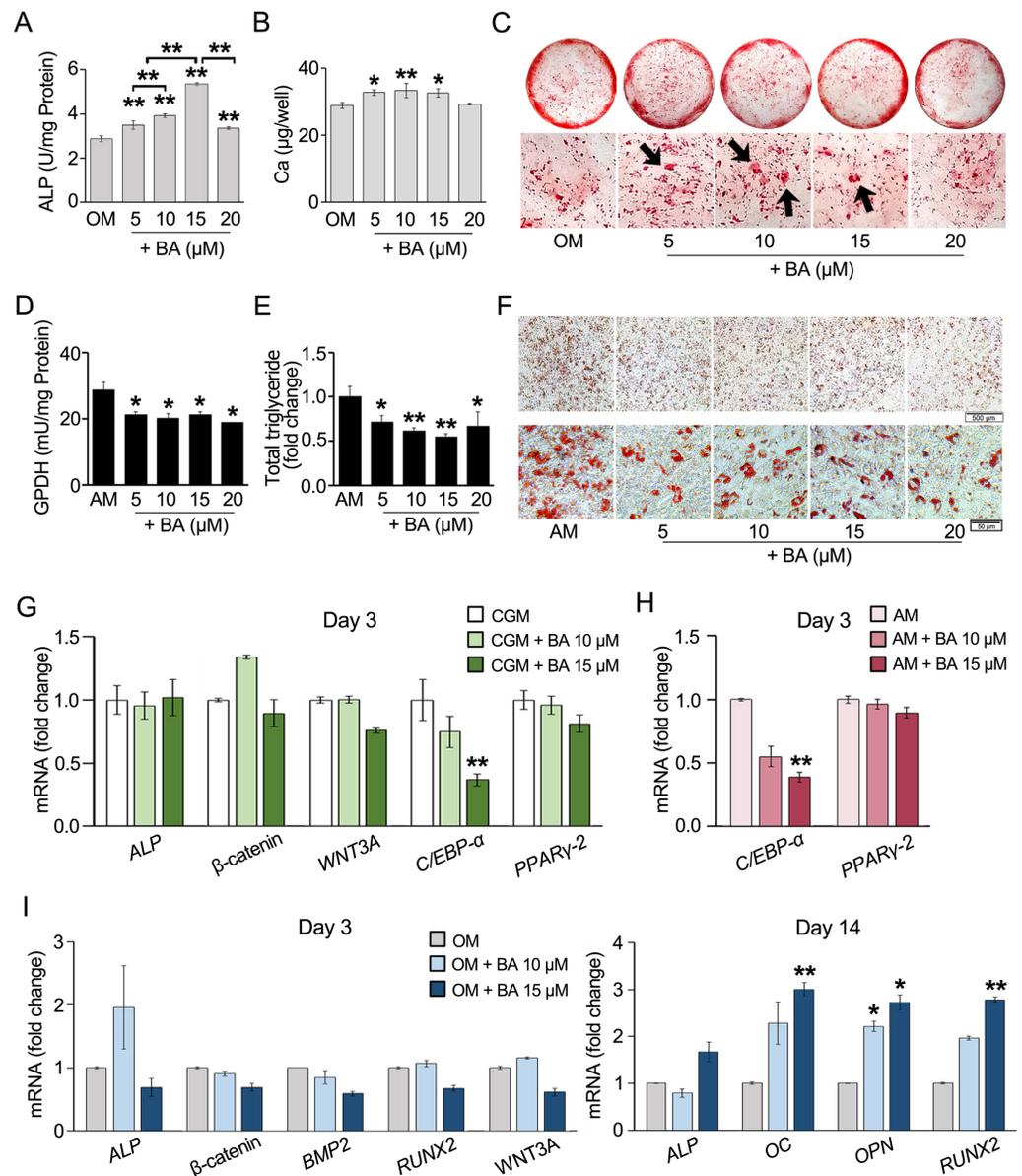
Figure 2 BA increased hMSC osteogenic differentiation but decreased hMSC adipogenic differentiation. For osteogenesis, ALP activity was analyzed on day 7 (A), whereas calcium deposition was assessed on day 14. Calcium was quantified with calcium colorimetric assays (B) and visualized for calcium nodule (arrows) with alizarin red staining (C). For adipogenesis, GPDH activity was analyzed on day 7 (D), whereas lipid droplet formation was stained with Oil Red O (F) and dissolved for quantification on day 21 (E). qRT-PCR analysis of hMSCs showed the effect of BA on the mRNA expressions of osteogenic and adipogenic markers during proliferating phase (G), adipogenic markers during adipogenesis (H), and osteogenic markers during osteogenesis (I). A, B, D, E $^*P < 0.05$ and $^{**}P < 0.01$. G, H, I statistical difference at $^*P < 0.05$, $^{**}P < 0.01$ and at least 2-fold changes.
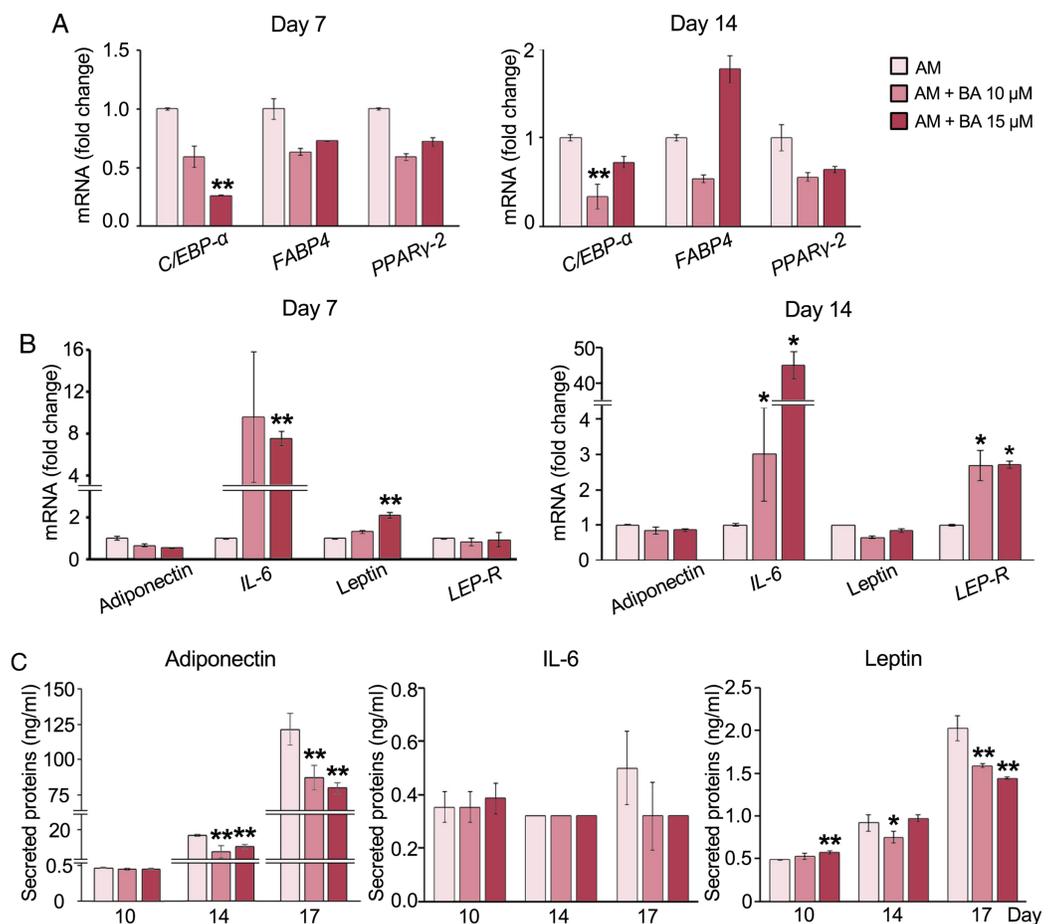
Figure 3 Effect of BA on white adipogenic markers and adipokine expressions on hMSCs. mRNA expressions of white adipocyte markers (A) and adipokines (B) were measured by qRT-PCR on days 7 and 14. The secreted adiponectin, IL-6, and leptin were measured with Milliplex Map Human Adipokine Magnetic Bead Panel Kits (C). Results are displayed as mean ± standard deviation ($n = 3$). $^*P < 0.05$ and $^{**}P < 0.01$.

BA down-regulated *C/EBP-α*, upregulated *IL-6* mRNA expression, but post- transcriptionally down-regulated adiponectin and leptin secretion in hMSCs

The decreased adipogenesis of hMSCs by BA with the downregulation of *C/EBP-α* expressions was remarkable at all time points on days 3, 7, and 14 (Figs. 2H and 3A), whereas the expressions of *PPARγ-2* and fatty acid-binding protein 4 (*FABP4*) were not significantly altered (Fig. 3A).

Further, adipokine mRNA expressions were analyzed with qRT-PCR. The result showed that BA at 15 µM significantly increased the expression of *IL-6* and leptin on day 7 (Fig. 3B). Meanwhile, the mRNA expressions of adiponectin and leptin-receptor (*LEP-R*), were not altered by BA on day 7 (Fig. 3B). On day 14, both *IL-6* and *LEP-R* expressions were significantly increased by BA at 10 and 15 µM, while the expressions of adiponectin and leptin were not altered (Fig. 3B).

Table 2 Adipokine secretions by hMSCs at day 14 showed the basal protein expressions of adiponectin, IL-6, leptin, and TNF-α (CGM) and their changes during adipogenic induction (AM).

Adipokine	Level of adipokine secretion	
	CGM (pg/ml)	AM (pg/ml)
Adiponectin	<13.91	19549.00
IL-6	340.15	0.32
Leptin	81.82	969.95
TNF-α	1.58	<0.40

Further, the secreted adipokines were analyzed with Milliplex Map Human Adipokine Magnetic Bead Panel Kits. The pilot results comparing the adipokines secreted by hMSCs during adipogenic and proliferating phases showed that the secretions of adiponectin and leptin were induced tremendously after 14 days in adipogenic induction media by about 1,400-and 11-fold, respectively (Table 2). On the contrary, the IL-6 secretion of hMSCs extensively decreased with adipogenic induction by more than 100-fold. TNF-α secretion was minimal during hMSC proliferation in the lower range of less than two pg/ml and diminished during adipogenesis (Table 2). We then analyzed the effect of BA during adipogenesis on hMSC-secreted adiponectin, IL-6, and leptin. The secreted adiponectin and leptin significantly decreased on days 14 and 17 with BA treatment (Fig. 3C). The secreted IL-6 was not altered by the addition of BA during adipogenesis (Fig. 3C).

BA potentially shifted adipogenic lineage differentiation of hMSCs toward brown adipocytes with increased glucose uptake and enhancement of *PPARγ* coactivator one alpha (*PGC-1α*) and uncoupling protein 1 (*UCP-1*) expressions

Recent studies showed that hMSCs can give rise to the distinctive lineages of white or brown adipocytes (*Park, Kim & Bae, 2014*). To determine the effect of BA on brown adipocyte formation, we analyzed lipid droplet formation and glucose uptake along with the mRNA expression of brown adipocyte markers.

The number of lipid droplets stained by Nile red were aligned with the results from Oil Red O staining. BA significantly reduced the amount of lipid droplets (Figs. 4A and 4C). Moreover, lipid droplet size distribution analysis revealed that BA decreased the ratio of large lipid droplets (>3 µm^2) and increased the ratio of small-sized lipid droplets (<1 µm^2) (Fig. 4B). A small lipid droplet size is one of the characters that can be used to distinguish brown adipocytes from white adipocytes (*Barneda et al., 2013*).

Glucose uptake by hMSCs was analyzed on days 10 and 14. The results showed that BA did not alter glucose uptake during adipogenesis of hMSCs on day 10 but significantly increased the glucose uptake on day 14 (Fig. 4E). Glucose transporter 4 (*GLUT4*) mRNA expression was quantified on days 7 and 14. The results showed that *GLUT4* expression was significantly increased by adipogenic induction on day 7 and decreased with BA treatment, while there was no change in GLUT4 expression on day 14 (Fig. 4D).

 10/19
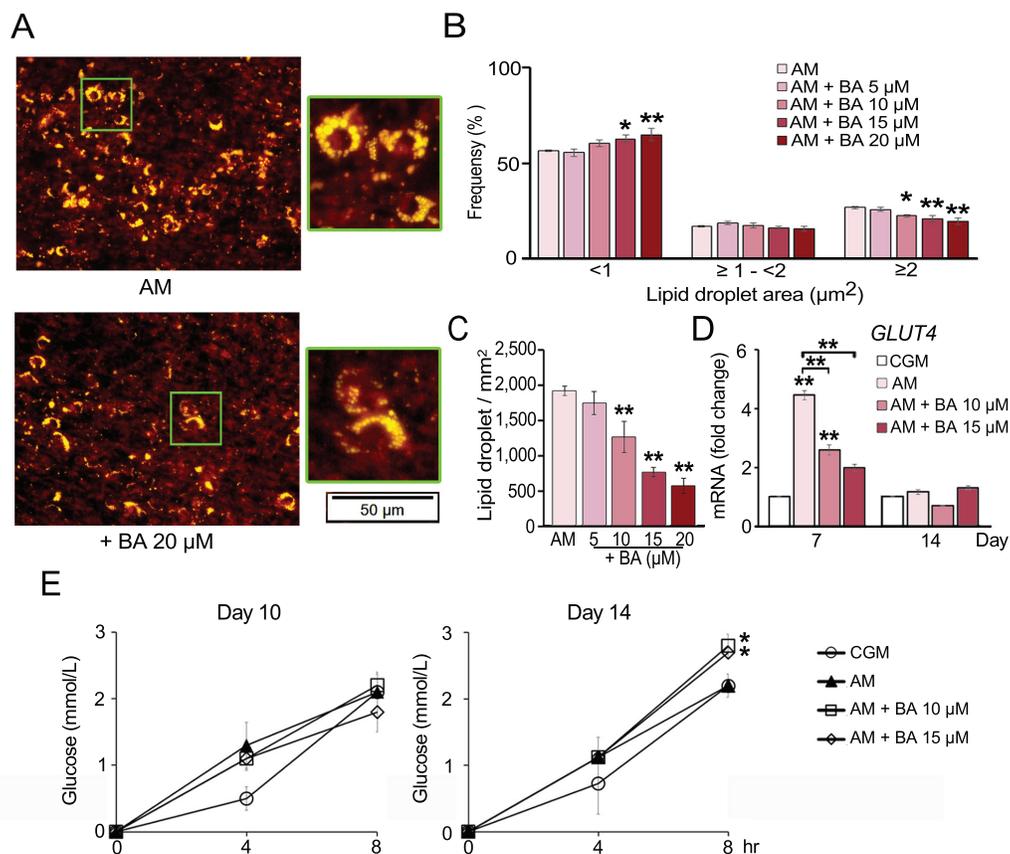
Figure 4 Effect of BA on hMSC lipid droplet formation and glucose uptake. Nile red staining showed reduction in the number (A and C) and size of lipid droplets (A and B). The mRNA expression of glucose transporter 4 (*GLUT4*) was quantified on days 7 and 14 (D). Glucose uptake of hMSCs was analyzed on days 10 and 14 (E). Results are displayed as mean ± standard deviation ($n = 3$). $^*P < 0.05$ and $^{**}P < 0.01$.

The expressions of five brown adipocyte markers, namely, bone morphogenetic protein 7 (*BMP7*), transcriptional co-regulator PR domain-containing 16 (*PRDM16*), myogenic factor 5 (*MYF5*), *PGC-1α*, and *UCP-1* were analyzed. The basal expression of maker genes during adipogenesis on day 7 showed that this hMSC cell line, UE7T-13, did not express *BMP7* nor *PRDM16* with a cycle threshold (Ct) over 35 (data not shown). Meanwhile, *MYF5*, *PGC-1α*, and *UCP-1* were normally expressed in hMSCs, BA enhanced the expressions of *PGC-1α* and *UCP-1* on day 7 by up to 6.42 and 3.22-fold, respectively (Fig. 5). On day 14, the expression of *PGC-1α* was not affected by BA, and the expression of *UCP-1* was decreased by BA at 10 μM.

DISCUSSION

Balancing cellular metabolisms by altering lipid synthesis and storage are intricate with diabetes causes and treatments. Cellular glucose uptake, lipid metabolism, adipose tissue formation, and energy utilization all play parts in balancing the blood glucose level. In addition, increasing the risk of osteoporosis and bone fractures have been associated
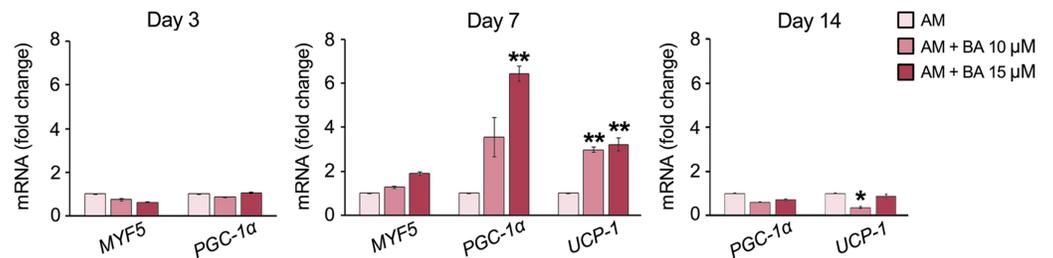
Figure 5 BA increased the expressions of brown adipogenic markers, *PGC-1α*, and *UCP-1* on day 7 of hMSC adipogenesis. Results are displayed as mean ± standard deviation ($n = 3$). *$P < 0.05$ and **$P < 0.01$.
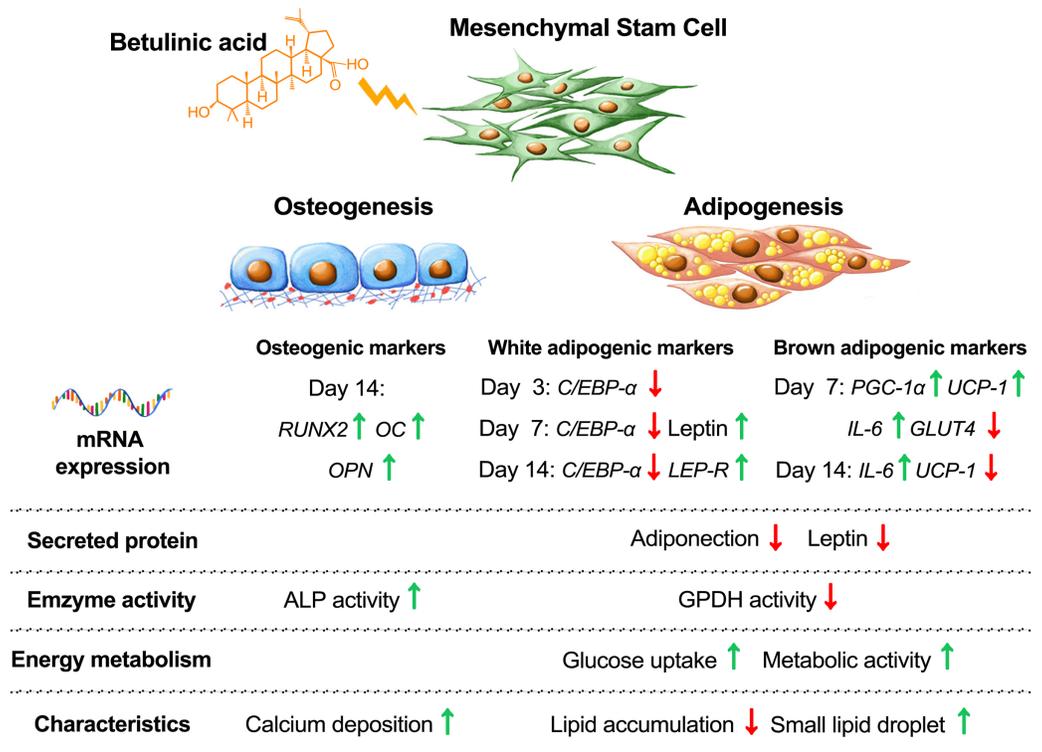
Figure 6 Concluding schematic shows how BA alters the fate of hMSC toward osteogenesis and brown adipogenesis and away from white adipogenesis.

with diabetes (*de Paula, Horowitz & Rosen, 2010*). In this study, we observed that BA attuned hMSC differentiation by increasing osteogenesis, decreasing white adipogenesis, and increasing brown adipogenesis with the upregulation of *UCP-1*, *PGC-1α*, and *IL-6* mRNA expressions, and post-transcriptional downregulation of adiponectin and leptin secretions (Fig. 6).

Hyperglycemia has direct and in-direct effects on bone formation and resorption by suppressing osteoblast cell growth and mineralization, increasing the number of osteoclasts, upregulating their markers, and inducing lipid formation within the bone marrow (*Wongdee & Charoenphandhu, 2011*). Increased risk of bone fracture was also reported when using the anti-diabetic drug, TZDs (*Chen et al., 2015*; *Schwartz & Sellmeyer,*

2007). Acting as the PPARγ agonist, this drug directly suppresses osteoblast development and induces bone loss (*Baroi et al., 2021*; *Jackuliak, Kužma & Payer, 2019*; *Takada et al., 2007*). On the contrary, the downregulation of the prime osteogenic regulator, *Runx2*, is also required for adipogenesis. The overexpression of *Runx2* can inhibit pre-adipocyte adipogenic differentiation and its trans-differentiation to bone cells (*Zhang et al., 2012*). In this study, we observed that BA increased hMSC osteogenesis by increasing the expression of *RUNX2*, *OC*, and *OPN* but did not directly alter the mRNA expression of *PPARγ* during adipogenesis. A previous study showed that BA can act as PPARγ antagonist by binding with PPAR receptors without transactivation activities (*Brusotti et al., 2017*).

Studies on synthetic PPAR antagonist showed that blocking or reducing the activity of PPARγ can reduce HFD-induced adipocyte hypertrophy and insulin resistance by reducing the size of adipocytes and decreasing the secretion of TNF-α and leptin (*Abbas et al., 2013*; *Rieusset et al., 2002*). However, the level of TNF-α secreted by hMSCs during adipogenesis in this study was below the detection limit. Thus, the effect of BA cannot be measured. The remarkable decrease in leptin secretion on day 17 by BA in hMSCs (Fig. 3C) without the decrease in leptin mRNA expression (Fig. 3B) suggested the effect of BA on secreted leptin at the levels of translation or secretion. Previous study on insulin treatment of adipose tissues from fed or starved rats also showed the changes in leptin secretion by altering leptin translation without alteration in leptin mRNA expression (*Lee et al., 2007*). Also, a decrease in leptin secretion in human adipose tissue by adrenergic activation was triggered at the level of leptin releasing from the preformed pool (*Ricci et al., 2005*).

BA has been extensively studied for its anti-cancer and anti-viral activities (*Moghaddam, Ahmad & Samzadeh-Kermani, 2012*). Recent studies showed its potential roles in balancing immunity and metabolisms including bone and lipid metabolisms (*Birgani et al., 2018*; *Mohsen et al., 2019*; *Ríos & Máñez, 2018*). It has been shown that BA reduced adipogenesis in mouse preadipocytes with decreases in *C/EBP-α, PPARγ, GLUT4*, cation diffusion facilitator, and perilipin one expressions (*Brusotti et al., 2017*). Also, BA increased glucose uptake rate in differentiated mouse adipocyte both with and without insulin stimulation (*Brusotti et al., 2017*). In this study, we also found that BA decreased the expressions of *C/EBP-α* and *GLUT4* while increased metabolic activity and glucose uptake in hMSCs during induced adipogenesis. After 11 weeks of BA treatment in HFD mice, BA helped maintain body temperature during acute cold exposure, decreased body weight, while increased brown fat tissues (*Kim et al., 2019*). Study of glucose overload in rat *in vivo* showed that BA helped maintain serum glucose level, increased serum insulin level, and increased muscle glycogen content (*Castro et al., 2014*). Further, *in vitro* study with dissected muscles showed that BA increased glucose uptake *via* increasing translocation of GLUT4 to plasma membrane (*Castro et al., 2014*). With BA increased metabolic activity and glucose uptake of hMSCs in our study and the new finding on BA improving energy balance with increase glucose uptake, and BAT formation in HFD mice (*Kim et al., 2019*), we then focused on the possibility of

BA driving hMSCs toward brown adipocytes rather than just suppressing white adipocyte formation.

The formation of white and brown adipocytes requires the regulation by PPARγ and C/EBP-α. These transcription factors play roles in the lipogenesis of white adipocytes and thermogenic program of brown adipocytes (*Inagaki, Sakai & Kajimura, 2016*; *Vernochet et al., 2009*). However, another gene coordination is required for brown adipogenic differentiation (*Kajimura, Seale & Spiegelman, 2010*). A recent study on the same hMSC line, UE7T-13, showed that modifying the expressions of endogenous gene *PRDM16* along with other key regulators, such as *PPARγ*, *C/EBP-α*, and Kruppel-like factor 5, by CRISPR-Cas9 can direct these hMSCs toward WAT or BAT formation (*Furuhata et al., 2017*). In this study, we observed that BA did not affect the expression of *PPARγ* but decreased the expression of *C/EBP-α* along with the upregulation of *UCP-1* and *PGC-1α*. Induced small lipid droplets formation by BA, the key characteristic of brown adipocytes, was also observed in this work. The study in HFD mice also showed that BA improved thermogenic capacity in acute cold exposure test with increased in brown fat gene expressions including *UCP-1* and *PGC-1α* (*Kim et al., 2019*). *UCP-1* and *PGC-1α* regulate the mitochondrial biogenesis, oxidative metabolism, and thermogenesis of BAT (*Park, Kim & Bae, 2014*). The activation of *UCP-1* provides benefits against obesity, decreases fat mass, and improve insulin sensitivity (*Li et al., 2000*; *Poher et al., 2015*). Overall, our findings suggest that BA can help with balanced glucose uptake and lipid metabolism during induced adipogenesis in hMSCs.

CONCLUSIONS

The present study examined the cellular responses of human mesenchymal stem cells, the progenitor cells of bone and fat tissues. The results suggested that betulinic acid increased osteogenesis and decreased adipogenesis in hMSCs. Decreases in leptin and adiponectin secretion were found at the secreted protein level but not at the mRNA expression. This indicated the potential control mechanisms of BA at the translation or cytokine releasing. Reduced size of lipid droplets along with the upregulation of UCP-1 and *PGC-1α* mRNA expressions suggested the potential effects of BA on brown adipogenic induction in human mesenchymal stem cells.

Funding

This work was supported by the Development and Promotion of Science and Technology Talents Project (DPST), Institute for the Promotion of Teaching Science and Technology, Thailand. The funders had no role in study design, data collection and analysis, decision to publish, or preparation of the manuscript.

Grant Disclosures

The following grant information was disclosed by the authors:
Institute for the Promotion of Teaching Science and Technology, Thailand.

Competing Interests

The authors declare that they have no competing interests.

Author Contributions

- Sasithon Senamontree performed the experiments, analyzed the data, prepared figures and/or tables, authored or reviewed drafts of the paper, and approved the final draft.
- Thitiporn Lakthan performed the experiments, authored or reviewed drafts of the paper, and approved the final draft.
- Pornsri Charoenpanich conceived and designed the experiments, authored or reviewed drafts of the paper, and approved the final draft.
- Chanpen Chanchao conceived and designed the experiments, authored or reviewed drafts of the paper, and approved the final draft.
- Adisri Charoenpanich conceived and designed the experiments, analyzed the data, authored or reviewed drafts of the paper, and approved the final draft.

Data Availability

The raw data of each replicate for all results are available in the Supplemental Files.

Supplemental Information

Supplemental information for this article can be found online at http://dx.doi.org/10.7717/peerj.12321#supplemental-information.

REFERENCES

Abbas S, Raza ST, Ahmed F, Ahmad A, Rizvi S, Mahdi F. 2013. Association of genetic polymorphism of PPARγ-2, ACE, MTHFR, FABP-2 and FTO genes in risk prediction of type 2 diabetes mellitus. *Journal of Biomedical Science* **20(1)**:1–8 DOI 10.1186/1423-0127-20-80.

Abdallah BM. 2017. Marrow adipocytes inhibit the differentiation of mesenchymal stem cells into osteoblasts via suppressing BMP-signaling. *Journal of Biomedical Science* **24(1)**:11 DOI 10.1186/s12929-017-0321-4.

Barneda D, Frontini A, Cinti S, Christian M. 2013. Dynamic changes in lipid droplet-associated proteins in the browning of white adipose tissues. *Biochimica Et Biophysica Acta (BBA)-Molecular and Cell Biology of Lipids* **1831(5)**:924–933 DOI 10.1016/j.bbalip.2013.01.015.

Baroi S, Czernik PJ, Chougule A, Griffin PR, Lecka-Czernik B. 2021. PPARG in osteocytes controls sclerostin expression, bone mass, marrow adiposity and mediates TZD-induced bone loss. *Bone* **147(11)**:115913 DOI 10.1016/j.bone.2021.115913.

Birgani GA, Ahangarpour A, Khorsandi L, Moghaddam HF. 2018. Anti-diabetic effect of betulinic acid on streptozotocin-nicotinamide induced diabetic male mouse model. *Brazilian Journal of Pharmaceutical Sciences* **54(2)**:425 DOI 10.1590/s2175-97902018000217171.

Brusotti G, Montanari R, Capelli D, Cattaneo G, Laghezza A, Tortorella P, Loiodice F, Peiretti F, Bonardo B, Paiardini A. 2017. Betulinic acid is a PPARγ antagonist that improves glucose uptake, promotes osteogenesis and inhibits adipogenesis. *Scientific Reports* **7(1)**:5777 DOI 10.1038/s41598-017-05666-6.

Cao JJ. 2011. Effects of obesity on bone metabolism. *Journal of Orthopaedic Surgery and Research* **6**:30 DOI 10.1186/1749-799X-6-30.

Castro AJG, Frederico MJS, Cazarolli LH, Bretanha LC, de Carvalho Tavares L, da Silva Buss Z, Dutra MF, de Souza AZP, Pizzolatti MG, Silva FRMB. 2014. Betulinic acid and 1, 25 (OH) 2 vitamin D3 share intracellular signal transduction in glucose homeostasis in soleus muscle. *The International Journal of Biochemistry & Cell Biology* **48**:18–27 DOI 10.1016/j.biocel.2013.11.020.

Chamberlain G, Fox J, Ashton B, Middleton J. 2007. Concise review: mesenchymal stem cells: their phenotype, differentiation capacity, immunological features, and potential for homing. *Stem Cells* **25(11)**:2739–2749 DOI 10.1634/stemcells.2007-0197.

Charoenpanich A, Wall ME, Tucker CJ, Andrews DMK, Lalush DS, Loboa EG. 2011. Microarray analysis of human adipose-derived stem cells in three-dimensional collagen culture: osteogenesis inhibits bone morphogenic protein and Wnt signaling pathways, and cyclic tensile strain causes upregulation of proinflammatory cytokine regulators and angiogenic factors. *Tissue Engineering Part A* **17(21–22)**:2615–2627 DOI 10.1089/ten.tea.2011.0107.

Chen H-H, Horng M-H, Yeh S-Y, Lin IC, Yeh C-J, Muo C-H, Sung F-C, Kao C-H. 2015. Glycemic control with thiazolidinedione is associated with fracture of T2DM patients. *PLOS ONE* **10(8)**:e0135530 DOI 10.1371/journal.pone.0135530.

Chen Y-YK, Khoury P, Ware JM, Holland-Thomas NC, Stoddard JL, Gurprasad S, Waldner AJ, Klion AD. 2014. Marked and persistent eosinophilia in the absence of clinical manifestations. *Journal of Allergy and Clinical Immunology* **133(4)**:1195–1202 DOI 10.1016/j.jaci.2013.06.037.

Choi H, Jeong BC, Kook MS, Koh JT. 2016. Betulinic acid synergically enhances BMP2-induced bone formation via stimulating Smad 1/5/8 and p38 pathways. *Journal of Biomedical Science* **23(1)**:45 DOI 10.1186/s12929-016-0260-5.

Costa JFO, Barbosa-Filho JM, de Azevedo Maia GL, Guimarães ET, Meira CS, Ribeiro-dos-Santos R, de Carvalho LCP, Soares MBP. 2014. Potent anti-inflammatory activity of betulinic acid treatment in a model of lethal endotoxemia. *International Immunopharmacology* **23(2)**:469–474 DOI 10.1016/j.intimp.2014.09.021.

de Melo CL, Queiroz MGR, Arruda Filho ACV, Rodrigues AM, de Sousa DF, Almeida JGL, Pessoa ODL, Silveira ER, Menezes DB, Melo TS. 2009. Betulinic acid, a natural pentacyclic triterpenoid, prevents abdominal fat accumulation in mice fed a high-fat diet. *Journal of Agricultural and Food Chemistry* **57(19)**:8776–8781 DOI 10.1021/jf900768w.

de Paula FJA, Horowitz MC, Rosen CJ. 2010. Novel insights into the relationship between diabetes and osteoporosis. *Diabetes/Metabolism Research and Reviews* **26(8)**:622–630 DOI 10.1002/dmrr.1135.

Deutsch MJ, Schriever SC, Roscher AA, Ensenauer R. 2014. Digital image analysis approach for lipid droplet size quantitation of oil red O-stained cultured cells. *Analytical Biochemistry* **445**:87–89 DOI 10.1016/j.ab.2013.10.001.

Furuhata Y, Nihongaki Y, Sato M, Yoshimoto K. 2017. Control of adipogenic differentiation in mesenchymal stem cells via endogenous gene activation using CRISPR-Cas9. *ACS Synthetic Biology* **6(12)**:2191–2197 DOI 10.1021/acssynbio.7b00246.

Grey A. 2009. Thiazolidinedione-induced skeletal fragility-mechanisms and implications. *Diabetes, Obesity and Metabolism* **11(4)**:275–284 DOI 10.1111/j.1463-1326.2008.00931.x.

Hogan AM, Swaminathan V, Pallegar NK, Christian SL. 2016. Nile red and 2-NBDG are incompatible for the simultaneous detection of lipid and glucose accumulation. *International Journal of Spectroscopy* **2016(7)**:1–8 DOI 10.1155/2016/5215086.

Inagaki T, Sakai J, Kajimura S. 2016. Transcriptional and epigenetic control of brown and beige adipose cell fate and function. *Nature Reviews Molecular Cell Biology* **17(8)**:480–495 DOI 10.1038/nrm.2016.62.

Jackuliak P, Kužma M, Payer J. 2019. Effect of antidiabetic treatment on bone. *Physiological Research* **68**(Suppl 2):S107–S120.

James AW. 2013. Review of signaling pathways governing MSC osteogenic and adipogenic differentiation. *Scientifica* **2013**(1):1–17 DOI 10.1155/2013/684736.

Jingbo W, Aimin C, Qi W, Xin L, Huaining L. 2015. Betulinic acid inhibits IL-1β-induced inflammation by activating PPAR-γ in human osteoarthritis chondrocytes. *International Immunopharmacology* **29**(2):687–692 DOI 10.1016/j.intimp.2015.09.009.

Kajimura S, Seale P, Spiegelman BM. 2010. Transcriptional control of brown fat development. *Cell Metabolism* **11**(4):257–262 DOI 10.1016/j.cmet.2010.03.005.

Kanawa M, Igarashi A, Ronald VS, Higashi Y, Kurihara H, Sugiyama M, Saskianti T, Pan H, Kato Y. 2013. Age-dependent decrease in the chondrogenic potential of human bone marrow mesenchymal stromal cells expanded with fibroblast growth factor-2. *Cytotherapy* **15**(9):1062–1072 DOI 10.1016/j.jcyt.2013.03.015.

Kim H-I, Moon S-H, Lee W-C, Lee H-J, Shivakumar SB, Lee S-H, Park B-W, Rho G-J, Jeon B-G. 2018. Inhibition of cell growth by cellular differentiation into adipocyte-like cells in dexamethasone sensitive cancer cell lines. *Animal Cells and Systems* **22**(3):178–188 DOI 10.1080/19768354.2018.1476408.

Kim KD, Jung HY, Ryu HG, Kim B, Jeon J, Yoo HY, Park CH, Choi BH, Hyun CK, Kim KT. 2019. Betulinic acid inhibits high-fat diet-induced obesity and improves energy balance by activating AMPK. *Nutrition, Metabolism and Cardiovascular Diseases* **29**(4):409–420 DOI 10.1016/j.numecd.2018.12.001.

Kubota N, Yamauchi T, Tobe K, Kadowaki T. 2006. Adiponectin-dependent and -independent pathways in insulin-sensitizing and antidiabetic actions of thiazolidinediones. *Diabetes* **55**(Supplement 2):S32–S38 DOI 10.2337/db06-S005.

Lacey DC, Simmons PJ, Graves SE, Hamilton JA. 2009. Proinflammatory cytokines inhibit osteogenic differentiation from stem cells: implications for bone repair during inflammation. *Osteoarthritis and Cartilage* **17**(6):735–742 DOI 10.1016/j.joca.2008.11.011.

Lee M-J, Yang R-Z, Gong D-W, Fried SK. 2007. Feeding and insulin increase leptin translation: importance of the leptin mRNA untranslated regions. *Journal of Biological Chemistry* **282**(1):72–80 DOI 10.1074/jbc.M609518200.

Lehmann JM, Moore LB, Smith-Oliver TA, Wilkison WO, Willson TM, Kliewer SA. 1995. An antidiabetic thiazolidinedione is a high affinity ligand for peroxisome proliferator-activated receptor γ (PPARγ). *Journal of Biological Chemistry* **270**(22):12953–12956 DOI 10.1074/jbc.270.22.12953.

Li B, Nolte LA, Ju J-S, Han DH, Coleman T, Holloszy JO, Semenkovich CF. 2000. Skeletal muscle respiratory uncoupling prevents diet-induced obesity and insulin resistance in mice. *Nature Medicine* **6**(10):1115–1120 DOI 10.1038/80450.

Lingaraju MC, Pathak NN, Begum J, Balaganur V, Ramachandra HD, Bhat RA, Ram M, Singh V, Kandasamy K, Kumar D. 2015. Betulinic acid attenuates renal oxidative stress and inflammation in experimental model of murine polymicrobial sepsis. *European Journal of Pharmaceutical Sciences* **70**:12–21 DOI 10.1016/j.ejps.2015.01.001.

Lo Y-C, Chang Y-H, Wei B-L, Huang Y-L, Chiou W-F. 2010. Betulinic acid stimulates the differentiation and mineralization of osteoblastic MC3T3-E1 cells: involvement of BMP/Runx2 and β-catenin signals. *Journal of Agricultural and Food Chemistry* **58**(11):6643–6649 DOI 10.1021/jf904158k.

Maxson S, Burg KJL. 2008. Conditioned media cause increases in select osteogenic and adipogenic differentiation markers in mesenchymal stem cell cultures. *Journal of Tissue Engineering and Regenerative Medicine* **2**:147–154 DOI 10.1002/(ISSN)1932-7005.

Moghaddam MG, Ahmad FBH, Samzadeh-Kermani A. 2012. Biological activity of betulinic acid: a review. *Journal of Pharmacy and Pharmacology* **3(2)**:119–123.

Mohamadnia AR, Shahbazkia HR, Sharifi S, Shafaei I. 2007. Bone-specific alkaline phosphatase as a good indicator of bone formation in sheepdogs. *Comparative Clinical Pathology* **16(4)**:265–270 DOI 10.1007/s00580-007-0692-0.

Mohsen GA-M, Abu-Taweel GM, Rajagopal R, Sun-Ju K, Kim H-J, Kim YO, Mothana RA, Kadaikunnan S, Khaled JM, Siddiqui NA, Al-Rehaily AJ. 2019. Betulinic acid lowers lipid accumulation in adipocytes through enhanced NCoA1-PPARγ interaction. *Journal of Infection and Public Health* **12(5)**:726–732 DOI 10.1016/j.jiph.2019.05.011.

Montazerolghaem M, Ning Y, Engqvist H, Ott MK, Tenje M, Mestres G. 2016. Simvastatin and zinc synergistically enhance osteoblasts activity and decrease the acute response of inflammatory cells. *Journal of Materials Science: Materials in Medicine* **27(2)**:23 DOI 10.1007/s10856-015-5639-4.

Murakami-Nishida S, Matsumura T, Senokuchi T, Ishii N, Kinoshita H, Yamada S, Morita Y, Nishida S, Motoshima H, Kondo T. 2019. Pioglitazone suppresses macrophage proliferation in apolipoprotein-E deficient mice by activating PPARγ. *Atherosclerosis* **286(1)**:30–39 DOI 10.1016/j.atherosclerosis.2019.04.229.

Nöth U, Osyczka AM, Tuli R, Hickok NJ, Danielson KG, Tuan RS. 2002. Multilineage mesenchymal differentiation potential of human trabecular bone-derived cells. *Journal of Orthopaedic Research* **20(5)**:1060–1069 DOI 10.1016/S0736-0266(02)00018-9.

Ou Z, Zhao J, Zhu L, Huang L, Ma Y, Ma C, Luo C, Zhu Z, Yuan Z, Wu J, Li R, Yi J. 2019. Anti-inflammatory effect and potential mechanism of betulinic acid on λ-carrageenan-induced paw edema in mice. *Biomedicine & Pharmacotherapy* **118**:109347 DOI 10.1016/j.biopha.2019.109347.

Park A, Kim WK, Bae K-H. 2014. Distinction of white, beige and brown adipocytes derived from mesenchymal stem cells. *World Journal of Stem Cells* **6(1)**:33 DOI 10.4252/wjsc.v6.i1.33.

Park SY, Kim HJ, Kim KR, Lee SK, Lee CK, Park KK, Chung WY. 2014. Betulinic acid, a bioactive pentacyclic triterpenoid, inhibits skeletal-related events induced by breast cancer bone metastases and treatment. *Toxicology and Applied Pharmacology* **275(2)**:152–162 DOI 10.1016/j.taap.2014.01.009.

Poher A-L, Veyrat-Durebex C, Altirriba J, Montet X, Colin DJ, Caillon A, Lyautey J, Rohner-Jeanrenaud F. 2015. Ectopic UCP1 overexpression in white adipose tissue improves insulin sensitivity in Lou/C rats, a model of obesity resistance. *Diabetes* **64(11)**:3700–3712 DOI 10.2337/db15-0210.

Quent VMC, Loessner D, Friis T, Reichert JC, Hutmacher DW. 2010. Discrepancies between metabolic activity and DNA content as tool to assess cell proliferation in cancer research. *Journal of Cellular and Molecular Medicine* **14(4)**:1003–1013 DOI 10.1111/j.1582-4934.2010.01013.x.

Rao X, Huang X, Zhou Z, Lin X. 2013. An improvement of the 2^ (–delta delta CT) method for quantitative real-time polymerase chain reaction data analysis. *Biostatistics, Bioinformatics and Biomathematics* **3(3)**:71–85.

Ricci MR, Lee M-J, Russell CD, Wang Y, Sullivan S, Schneider SH, Brolin RE, Fried SK. 2005. Isoproterenol decreases leptin release from rat and human adipose tissue through posttranscriptional mechanisms. *American Journal of Physiology-Endocrinology and Metabolism* **288(4)**:E798–E804 DOI 10.1152/ajpendo.00446.2004.

Rieusset J, Touri F, Michalik L, Escher P, Desvergne B, Niesor E, Wahli W. 2002. A new selective peroxisome proliferator-activated receptor γ antagonist with antiobesity and antidiabetic activity. *Molecular Endocrinology* **16(11)**:2628–2644 DOI 10.1210/me.2002-0036.

Ríos JL, Máñez S. 2018. New pharmacological opportunities for betulinic acid. *Planta Medica* **84(1)**:8–19 DOI 10.1055/s-0043-123472.

Samuel S, Ahmad RE, Ramasamy TS, Karunanithi P, Naveen SV, Kamarul T. 2019. Platelet-rich concentrate in serum-free medium enhances cartilage-specific extracellular matrix synthesis and reduces chondrocyte hypertrophy of human mesenchymal stromal cells encapsulated in alginate. *Platelets* **30(1)**:66–74 DOI 10.1080/09537104.2017.1371287.

Sardone LD, Renlund R, Willett TL, Fantus IG, Grynpas MD. 2011. Effect of rosiglitazone on bone quality in a rat model of insulin resistance and osteoporosis. *Diabetes* **60**:3271–3278.

Schwartz AV, Sellmeyer DE. 2007. Thiazolidinedione therapy gets complicated: is bone loss the price of improved insulin resistance? *Diabetes Care* **30**:1670–1671.

Sellmeyer DE, Civitelli R, Hofbauer LC, Khosla S, Lecka-Czernik B, Schwartz AV. 2016. Skeletal metabolism, fracture risk, and fracture outcomes in type 1 and type 2 diabetes. *Diabetes* **65**:1757–1766.

Song T-J, Park C-H, In K-R, Kim J-B, Kim JH, Kim M, Chang HJ. 2021. Antidiabetic effects of betulinic acid mediated by the activation of the AMP-activated protein kinase pathway. *PLOS ONE* **16(4)**:e0249109 DOI 10.1371/journal.pone.0249109.

Sonowal H, Kumar A, Bhattacharyya J, Gogoi PK, Jaganathan BG. 2013. Inhibition of actin polymerization decreases osteogeneic differentiation of mesenchymal stem cells through p38 MAPK pathway. *Journal of Biomedical Science* **20(1)**:71 DOI 10.1186/1423-0127-20-71.

Sottile V, Seuwen K. 2001. A high-capacity screen for adipogenic differentiation. *Analytical Biochemistry* **293(1)**:124–128 DOI 10.1006/abio.2001.5121.

Takada I, Suzawa M, Matsumoto K, Kato S. 2007. Suppression of PPAR transactivation switches cell fate of bone marrow stem cells from adipocytes into osteoblasts. *Annals of the New York Academy of Sciences* **1116(1)**:182–195 DOI 10.1196/annals.1402.034.

Tsujimura M, Kusamori K, Nishikawa M. 2019. Rapid regulation of human mesenchymal stem cell proliferation using inducible caspase-9 suicide gene for safe cell-based therapy. *International Journal of Molecular Sciences* **20(22)**:5759 DOI 10.3390/ijms20225759.

Tu B, Peng ZX, Fan QM, Du L, Yan W, Tang TT. 2014. Osteosarcoma cells promote the production of pro-tumor cytokines in mesenchymal stem cells by inhibiting their osteogenic differentiation through the TGF-β/Smad2/3 pathway. *Experimental Cell Research* **320(1)**:164–173 DOI 10.1016/j.yexcr.2013.10.013.

Vernochet C, Peres SB, Davis KE, McDonald ME, Qiang L, Wang H, Scherer PE, Farmer SR. 2009. C/EBPα and the corepressors CtBP1 and CtBP2 regulate repression of select visceral white adipose genes during induction of the brown phenotype in white adipocytes by peroxisome proliferator-activated receptor γ agonists. *Molecular and Cellular Biology* **29(17)**:4714–4728 DOI 10.1128/MCB.01899-08.

Walker JM. 1996. *The protein protocols handbook*. Berlin: Springer Science & Business Media.

Wongdee K, Charoenphandhu N. 2011. Osteoporosis in diabetes mellitus: possible cellular and molecular mechanisms. *World Journal of Diabetes* **2(3)**:41 DOI 10.4239/wjd.v2.i3.41.

Zhang N, Hu X, He S, Ding W, Wang F, Zhao Y, Huang Z. 2019. LncRNA MSC-AS1 promotes osteogenic differentiation and alleviates osteoporosis through sponging microRNA-140-5p to upregulate BMP2. *Biochemical and Biophysical Research Communications* **519(4)**:790–796 DOI 10.1016/j.bbrc.2019.09.058.

Zhang Y-Y, Li X, Qian S-W, Guo L, Huang H-Y, He Q, Liu Y, Ma C-G, Tang Q-Q. 2012. Down-regulation of type I Runx2 mediated by dexamethasone is required for 3T3-L1 adipogenesis. *Molecular Endocrinology* **26(5)**:798–808 DOI 10.1210/me.2011-1287.